Articles

Interaction of a Mitochondrial Presequence with Lipid Membranes: Role of Helix Formation for Membrane Binding and Perturbation†

Torsten Wieprecht,*,‡ Ognjan Apostolov,‡ Michael Beyermann,§ and Joachim Seelig‡

Department of Biophysical Chemistry, Biocenter of the University of Basel, Klingelbergstr. 70, CH-4052 Basel, Switzerland, Institute of Molecular Pharmacology, Alfred-Kowalke Strasse 4, D-10315 Berlin, Germany

Received July 28, 2000; Revised Manuscript Received October 3, 2000

ABSTRACT: The binding of a peptide to a biological membrane is often accompanied by a transition from a random coil structure to an amphipathic α-helix. Recently, we have presented a new approach which allows the determination of the thermodynamic parameters of membrane-induced helix formation [Wieprecht et al. (1999) *J. Mol Biol. 294,* 785]. It involves a systematic variation of the helix content of a given peptide by double D-substitution and a correlation of the binding parameters with the helicity. Here we have used this method to study membrane-induced helix formation for the presequence of rat mitochondrial rhodanese (RHD). The thermodynamic parameters of binding of the peptide RHD and of four of its double D-isomers were determined for 30 nm (SUVs) and 100 nm (LUVs) unilamellar vesicles composed of phosphatidylcholine/phosphatidylglycerol (3:1) using circular dichroism spectroscopy, fluorescence spectroscopy, and isothermal titration calorimetry. The incremental changes of the thermodynamic parameters of helix formation were found to be very similar for SUVs and LUVs. Membrane-induced helix formation of RHD entailed a negative enthalpy of $\Delta H_{helix} = -0.5$ to -0.6 kcal/mol/residue and was opposed by an entropy of about $\Delta S_{helix} = -1$ to -1.4 cal/mol K/residue. The free energy of helix formation, ΔG_{helix}, was about -0.2 kcal/mol, and helix formation accounted for 50−60% of the total free energy of membrane binding. Dye-release experiments were used to assess the role of helix formation for the membrane perturbation potential of the peptides. While helix formation plays a major role for membrane binding, it appears to have little importance for inducing membrane leakiness.

The binding of peptides and proteins to biological membranes is often accompanied by a random coil → α-helix transition. This process is particularly favored if the resulting helix is amphipathic (*1*). In an amphipathic helix, the hydrophobic amino acid side chains insert into the hydrophobic membrane interior, while the hydrophilic residues remain in contact with the polar headgroups. Typical examples for peptides and proteins undergoing a membrane-induced random coil → α-helix transition are antibacterial and hemolytic peptides, virus fusion peptides, signal peptides for protein import or export and apolipoproteins (*1*−*8*).

We have recently described a new approach for the thermodynamic analysis of the membrane-induced random coil → α-helix transition using the amphipathic antibacterial peptide magainin 2 amide (M2a)[1] as a model system (*9*). The parent peptide M2a was compared with three double D-isomers of M2a, where two adjacent amino acids within the sequence were substituted by their corresponding D-enantiomers. Double D-substitution results in a local disturbance of the α-helical conformation without modifying other important peptide properties such as the side chain functionality and the peptide hydrophobicity (*3*, *10*). By measuring the binding of these peptides to small unilamellar vesicles (SUVs) and correlating the thermodynamic binding parameters with the helicity, the incremental contribution of helix formation to the thermodynamic binding parameters could be derived. Helix formation was driven by a negative enthalpy change, ΔH_{helix}, of -0.7 kcal/mol/residue and opposed by a negative entropy change, ΔS_{helix}, of -1.9 cal/mol K. The standard free energy of helix formation, ΔG_{helix}, was -0.14 kcal/mol/residue and accounted for about 50% of the free energy of binding. Recently, we have repeated the experiments with large unilamellar vesicles (LUVs) which are less curved than SUVs and resemble biological membranes more closely. The parameters of helix formation were almost identical for SUVs and LUVs (*11*).

At present, the M2a system is the only peptide for which a full set of parameters is available. A binding comparison

† Supported by the Swiss National Science Foundation Grant 31-42058.94

* To whom correspondence should be addressed. Phone: +41-61-267-2190. Fax: +41-61-267-2192. E-mail: torsten.wieprecht@unibas.ch.

‡ Biocenter of the University of Basel.

§ Institute of Molecular Pharmacology.

[1] Abbreviations: SUV, small unilamellar vesicle; LUV, large unilamellar vesicle; M2a, magainin 2 amide; RHD, peptide corresponding to the presequence of mitochondrial rhodanese; POPC, 1-palmitoyl-2-oleoyl-*sn*-glycero-3-phosphocholine; POPG, 1-palmitoyl-2-oleoyl-*sn*-glycero-3-phosphoglycerol; CD, circular dichroism; ITC, isothermal titration calorimetry; Tris, tris(hydroxymethyl) aminomethane.

10.1021/bi001774v CCC: $19.00
Published on Web 11/23/2000

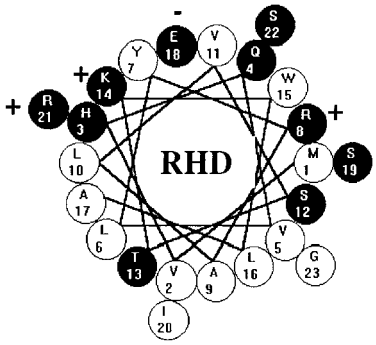

FIGURE 1: Helical wheel projection and amino acid sequence of the presequence of rat mitochondrial rhodanese (RHD). The one letter code is used to designate amino acid residues. White circles refer to hydrophobic and black circles to hydrophilic residues.

has been made for melittin and an incremental free energy of helix formation, ΔG_{helix}, of -0.4 kcal/mol/residue (but no ΔH_{helix}) was derived (*12*). In contrast, systematic studies of apolipoproteins led to a ΔH_{helix} of -1.3 kcal/mol/residue (but no ΔG_{helix}) (*13*).

Because of considerable variation in the few data available, we have extended the double D-substitution approach to the presequence of rat mitochondrial rhodanese, which has a different biological function than the membrane-permeabilizing magainin. Mitochondrial rhodanese is an enzyme synthesized in the cytosol and subsequently transported across the mitochondrial membranes (*14*). The N-terminal presequence is required for protein translocation and acts as a targeting signal for the complex proteinaceous import machinery located in the outer and inner mitochondrial membrane (*15*). Mitochondrial presequences of different proteins possess a low sequence similarity but are generally positively charged and are capable of assuming an amphipathic α-helical conformation (*4*, *16*). Apart from the interaction with the proteinaceous machinery, the interaction of presequences with the lipid matrix of the mitochondrial membrane was shown to contribute to protein import (*4*, *15*). It was suggested that interaction of the presequence with the membrane induces an α-helix formation thereby facilitating binding to the import machinery (*4*, *17*−*19*). The 23-amino acid presequence of rat mitochondrial rhodanese (RHD) was previously shown to assume a random coil in water but to fold into an amphipathic α-helix upon binding to a lipid bilayer (*6*, *20*) (Figure 1).

In this work, we have synthesized RHD and four of its double D-isomers (d2,3 RHD; d4,5 RHD; d11,12 RHD; d18,-19 RHD) and have measured their interaction with negatively charged 1-palmitoyl-2-oleoyl-*sn*-glycero-3-phosphocholine/1-palmitoyl-2-oleoyl-*sn*-glycero-3-phosphoglycerol [POPC/POPG (3:1)] vesicles. The conformations of the peptides in solution and bound to lipid vesicles were studied using circular dichrosism (CD) spectroscopy. We have determined the binding parameters by means of spectroscopic methods (CD and fluorescence spectroscopy) and isothermal titration calorimetry (ITC) and have correlated them with the helicity of the membrane-bound peptides. Binding studies were performed with both small (SUVs) and large (LUVs) unilamellar vesicles in order to elucidate the differences between the two frequently used model systems. Since signal peptides are also known to perturb the membrane, the ability of the individual RHD analogues to permeabilize vesicles was measured and was correlated with the helicity of the peptides.

EXPERIMENTAL PROCEDURES

Materials. POPC and POPG were purchased from Avanti Polar Lipids. Inc., Alabaster, AL. The Fmoc amino acids for peptide synthesis were obtained from Novabiochem, Bad Soden, Germany. All other chemicals were of analytical or reagent grade. Buffer was prepared from 18 MΩ water obtained from a NANOpure A filtration system.

Peptide Synthesis. RHD and its double D-isomers were synthesized by solid-phase methods using standard Fmoc chemistry on Tenta Gel S RAM resin (0.21 mmol/g; RAPP Polymere, Tübingen, Germany) in the continuous-flow mode on a MilliGen 9050 (Millipre, MA) peptide synthesizer. Purification was carried out by preparative high-performance liquid chromatography (HPLC) on PolyEncap A300, 10 μm (250 × 20 mm i.d.) (Bischoff Analyzentechnik GmbH, Leonberg, Germany) to give final products >95% pure by HPLC analysis. All peptides were characterized by matrix-assisted laser desorption ionization mass spectrometry (MALDI II; Kratos, Manchester, U.K.) with peptide content of lyophilized samples being determined by quantitative amino acid analysis (LC 3000, Biotronik-Eppendorf, Germany).

Preparation of Vesicles. A defined amount of lipid in chloroform was first dried under nitrogen. The lipid was dissolved in dichloromethane and then again dried under nitrogen and, subsequently, overnight under high vacuum. Typically, 2−3 mL of buffer (10 mM Tris, 100 mM NaCl, pH 7.4) were added to the lipid and the dispersion was extensively vortexed. For preparation of small unilamellar vesicles (SUVs) the lipid dispersion was sonified (in ice−water) using a titanium tip ultrasonicator until the solution became transparent. Titanium debris was removed by centrifugation (Eppendorf tabletop centrifuge, 10 min at 14 000 rpm).

LUVs were prepared by the extrusion technique (*21*). The lipid suspension was frozen and thawed in liquid nitrogen (six times) and extruded through polycarbonate filters. (at least 10 times through two stacked 0.1 μm filters). The lipid concentration was calculated on basis of the weight of the dried lipid for SUVs as well as LUVs.

LUVs for dye release experiments were prepared as described above using calcein containing buffer (70 mM calcein and 10 mM Tris, pH 7.4). After preparation, the untrapped calcein was removed from the vesicles by gel filtration on a Sephadex G75 column (eluent: buffer containing 10 mM Tris, 100 mM NaCl, pH 7.4). The lipid concentration was determined by quantitative phosphorus analysis (*22*).

High Sensitivity Titration Calorimetry. Isothermal titration calorimetry was performed using a MicroCal Omega high-sensitivity titration calorimeter (Microcal, Norhampton, MA) (*23*). Solutions were degassed under vacuum prior to use. The calorimeter was calibrated electrically. The heats of dilution were determined in control experiments by injecting either peptide solution or lipid suspension into buffer. The heats of dilution were subtracted from the heats determined in the corresponding peptide-lipid binding experiments.

Circular Dichroism Spectroscopy. CD measurements of the peptides in buffer (10 mM Tris and 100 mM NaCl, pH

7.4), trifluoroethanol (TFE)/buffer, or the presence of SUVs (same buffer) were carried out on a Jasco 720 spectrometer between 200 and 260 nm at 30 °C. Minor contributions of circular dichroism and circular differential scattering of the SUVs were eliminated by subtracting the lipid spectra of the corresponding peptide-free suspensions. The helicity of the peptides, f_h, was determined from the mean residue ellipticity [Θ] at 222 nm:

$$f_h = \frac{[\Theta]_{222} - [\Theta]_{coil}}{[\Theta]_{helix} - [\Theta]_{coil}} \quad (1a)$$

where $[\Theta]_{222}$ is the measured mean residue ellipticity at 222 nm (deg cm^2 dmol^{-1}), and $[\Theta]_{helix}$ and $[\Theta]_{coil}$ are the mean residue ellipticities (at 222 nm) of the completely helical and completely coiled form of the peptide, respectively. $[\Theta]_{helix}$ was calculated according to ref *24*:

$$[\Theta]_{helix} = \left[-4000\left(1 - \frac{2.5}{n}\right) + 100T\right]\frac{\text{deg cm}^2}{\text{dmol}} \quad (1b)$$

where n is the number of amino acid residues and T is the temperature (°C). $[\Theta]_{coil}$ was assumed to be −1500 deg cm^2 dmol^{-1} and corresponds to the ellipticity of d18,19 RHD in buffer (lowest ellipticity measured).

Fluorescence Spectroscopy. Tryptophan fluorescence spectra of peptide−vesicle mixtures were measured on a Jasco FP 777 spectrofluorometer in a stirred 1 cm cuvette thermostated at 30 °C (peptide concentrations: 3−10 μM, lipid concentrations: 0−10 mM). The excitation wavelength was set to 280 nm and fluorescence emission was recorded between 300 and 450 nm. The excitation slit width was 3 nm and the emission slit width was between 3 and 5 nm depending on the peptide concentration. The background intensity of the vesicles was measured in separate control experiments without peptide and was subtracted from the peptide fluorescence spectra. The intensity of the resulting spectra was corrected for the inner filter effect using the method of Lakowicz (*25*).

Dye Release Experiments. Aliquots of a calcein-containing LUV suspension (10−20 μL) were injected into a cuvette containing 2.5 mL of a stirred thermostated peptide solution of defined concentration (final lipid concentration was 50 μM). Calcein release from LUVs was determined fluorometrically by measuring the decrease in self-quenching (excitation at 490 nm, emission at 520 nm) on a Jasco FP 777 spectrofluorometer. The fluorescence intensity corresponding to 100% calcein release was determined by addition of 100 μL of 10% Triton X-100 solution.

RESULTS

Secondary Structure of RHD Peptides. The conformations of RHD and its double D-isomers were studied in buffer (10 mM Tris and 100 mM NaCl, pH 7.4), in trifluoroethanol (TFE) and in the presence of POPC/POPG (3:1) SUVs at 30 °C. In buffer, the helicity of the peptides was below 5% and the spectra were typical for random coil structures (Table 1). In presence of 50% TFE, a solvent frequently used to assess the α-helix propensity of peptides, the spectra of all analogues were characterized by the helix double minimum at 222 and 208 nm (not shown). The helicity of the all-L peptide was calculated to be ∼79%, but those of the double D-isomers were distinctly lower. The lowest helicity was measured for the d11,12 RHD analogue (51%), where the D-amino acids were introduced in the middle of the sequence (Table 1). The addition of negatively charged POPC/POPG (3:1) SUVs also resulted in α-helix formation of the peptides. Under the conditions employed (8−25 μM peptide; 2−10 mM lipid), the peptides RHD, d2,3 RHD, d4,5 RHD, and d11,12 RHD were completely bound to the vesicles as determined from the binding isotherms (cf. below) and the CD spectra could be assigned exclusively to the conformation of the lipid-bound peptide. For d18,19 RHD only about 90% of the peptide was lipid-bound and a correction for incomplete binding was necessary. The extent of helix formation of the lipid-bound peptides is summarized in Table 1. The helicity of the parent peptide was 70%, in agreement with results previously reported for RHD bound to L-α-lecithin/cardiolipin SUVs (*6*). Double D-substitution in position 2,3 had only a minor effect on helicity. However, substitution in the other positions distinctly decreased the helicity of the lipid-bound peptides by about 26−28%.

Table 1: Helicity of RHD Peptides in Buffer and TFE/Buffer and Bound to POPC/POPG (3:1) SUVs and Fluorescence Maximum of Peptides Bound to POPC/POPG(3:1) LUVs at 30 °C[a]

peptide	buffer[b] (%)	TFE/buffer (1:1)[c] (%)	POPC/POP (3:1)[d] (%)	fluorescence maximum (nm)
RHD	4	79	70	342
d2,3 RHD	3	70	67	342
d4,5 RHD	3	63	44	340
d11,12 RHD	2	51	43	337
d18,19 RHD	0	58	42	336

[a] The helicity was calculated from the mean residue ellipticity at 222 nm according to ref *24*. [b] The peptide concentration was between 12 and 27 μM (buffer, 10 mM Tris and 100 mM NaCl, pH 7.4). [c] The peptide concentration was between 9 and 16 μM (buffer, 10 mM Tris and 100 mM NaCl, pH 7.4). [d] Small unilamellar vesicles were used for CD experiments. The lipid concentration was between 2 and 10 mM and the peptide concentration between 8 and 25 μM. The helicity is corrected for incomplete peptide binding (cf. text).

Binding Isotherms of RHD Peptides for POPC/POPG (3:1) Vesicles. Binding isotherms of RHD peptides were measured for POPC/POPG (3:1) SUVs and LUVs at 30 °C. The distinct conformational differences between the peptides in buffer (random coil) and in the presence of SUVs (α-helix) allowed the determination of the binding isotherms by means of CD spectroscopy. CD spectra of peptide solutions (c^0_{pep} between 7 and 27 μM) were recorded in the presence of varying amounts of POPC/POPG (3:1) SUVs at 30 °C (lipid/peptide ratio between 0 and 600, depending on the lipid affinity). Without lipid, the measured ellipticity at 222 nm reflects the conformation of the peptide in aqueous solution (Θ_W). The ellipticity decreases with increasing lipid concentration, c_L, until it approaches a constant level at a lipid-to-peptide ratio where virtually all the peptide is bound to the membrane (Θ_M). The limiting lipid-to-peptide ratio depends on the lipid affinity and is different for the individual analogues. At lower lipid-to-peptide ratios the mole fraction of bound peptide, $X_{P,b}$, is given by

$$X_{P,b} = (\Theta - \Theta_W)(\Theta_M - \Theta_W) \quad (2)$$

where Θ is the measured ellipticity. The concentration of peptide remaining free in solution, c_f, is The molar ratio of

$$c_f = c^0_{pep}\,(1 - X_{P,b}) \quad (3)$$

bound peptide per lipid, X_b, is calculated as

$$X_b = \frac{c_b}{c_L} = \frac{X_{P,b}c^0_{pep}}{c_L} \quad (4)$$

where c_L is the total lipid concentration.

A plot of X_b vs c_f, determined for different peptide-to-lipid ratios, yields the binding isotherm. The binding isotherms of RHD and its double D-analogues for POPC/POPG (3:1) SUVs are shown in Figure 2. For the conditions used, all analogues were found to permeabilize POPC/POPG (3:1) membranes (cf. below, dye release experiments). For amphipathic peptides membrane permeabilization is generally coupled to a peptide translocation from the outer to the inner leaflet of the vesicles (*26*, *27*). The binding isotherms were therefore calculated on basis of the total lipid concentration (lipid in outer layer + inner layer). Figure 2 demonstrates that the lipid affinity of the peptides is highest for the helical peptides RHD and d2,3 RHD, but distinctly lower for the less helical analogues d4,5 RHD, d11,12 RHD, and d18,19 RHD.

The binding isotherms can be explained with a *surface partition* equilibrium, in which peptide binding is linearly related to the peptide concentration immediately above the membrane surface (surface concentration, c_M).

$$X_b = Kc_M \quad (5)$$

The model was previously used to describe binding of a multitude of differently charged molecules to lipid membranes and is discussed in detail elsewhere (*28*, *29*).

In short, the surface concentration, c_M, depends (i) on the free peptide concentration in bulk solution, c_f, (ii) on the peptide charge, and (iii) on the membrane surface potential. POPC/POPG (3:1) vesicles have a negative surface potential leading to an attraction of the cationic RHD peptides ($z \approx +2.5$) from bulk solution to the membrane surface. Consequently, the peptide concentration near the membrane surface (c_M) is enhanced compared to that in bulk solution (c_f). Using the Gouy−Chapman theory (for reviews see refs *30*−*32*), it is possible to calculate c_M for each data point of the binding isotherm and to determine the binding constant K. The solid lines in Figure 2 are the best theoretical fits to the experimental data and the corresponding binding constants are listed in Table 2. Na^+ binding to negatively charged PG was included with a binding constant of $K_{Na+} = 0.6\ M^{-1}$. The binding constants of the peptides are the mean of two independent measurements of the binding isotherms. From the binding constants K, the standard free energy of binding $\Delta G°$ can be calculated according to

$$\Delta G^0 = -RT \ln 55.5\,K \quad (6)$$

where the factor 55.5 is the molar concentration of water and corrects for the cratic contribution (*33*) (Table 2).

CD spectroscopy cannot be used to determine binding isotherms of peptides to LUVs, because of increased scattering effects. Therefore, the intrinsic tryptophan fluorescence (Trp^{15}) of the peptides was employed to derive binding isotherms for LUVs. In addition to Trp^{15}, tyrosine (Tyr^7) is also excited at the excitation wavelength of 280 nm. The resulting fluorescence spectra hence represent the summed tryptophan and tyrosine fluorescence, with the tryptophan fluorescence clearly dominating the shape and intensity of the spectra. Binding of RHD peptides to POPC/POPG (3:1) LUVs results in a distinct blue shift of the fluorescence maximum (from 354 nm in buffer to 342−336 nm, depending on the double D-substitution site, see Table 1) as well as in an increase in the fluorescence intensity. These spectroscopic changes are typical for a transfer of the tryptophan residue from an aqueous environment into a more hydrophobic phase (*25*). To measure the binding isotherm,

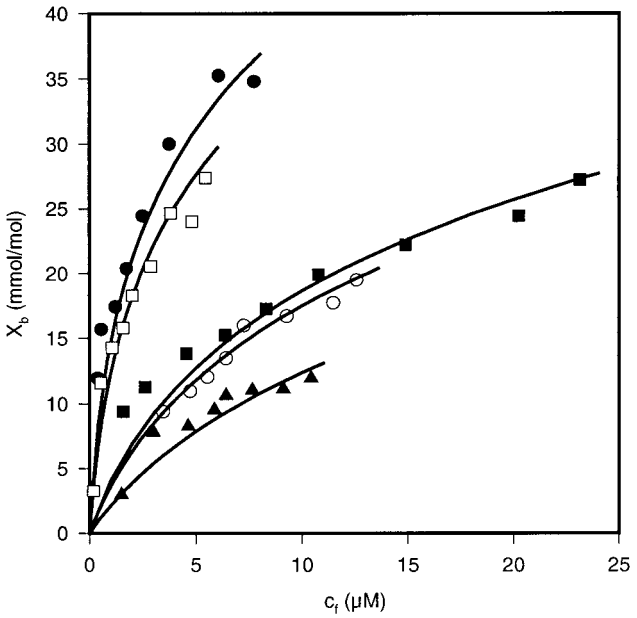

FIGURE 2: Binding isotherms of RHD and its double D-isomers for POPC/POPG (3:1) SUVs at 30 °C (buffer, 10 mM Tris and 100 mM NaCl, pH 7.4): (●) RHD, (□) d2,3 RHD, (○) d4,5 RHD, (■) d11,12 RHD, (▲) d18,19 RHD. Isotherms were determined by CD spectroscopy. The solid lines correspond to the theoretical binding isotherms calculated by combining a surface partition equilibrium with the Gouy−Chapman theory in order to correct for the electrostatic effect.

Table 2: Thermodynamic Parameters of Binding of RHD Peptides to POPC/POPG(3:1) SUVs and LUVs at 30 °C

peptide	K[a] (M^{-1})	$\Delta G°$[b] (kcal/mol)	$\Delta H°$[c] (kcal/mol)	$\Delta S°$[d] (cal/molK)
LUVs[e]				
RHD	160	−5.5	−1.7	12.4
d2,3 RHD	115	−5.3	0.5	19.0
d4,5 RHD	18	−4.2	3.1	23.9
d11,12 RHD	15	−4.0	1.4	18.0
d18,19 RHD	22	−4.3	3.8	26.6
SUVs[f]				
RHD	245	−5.7	−14.9	−30.3
d2,3 RHD	180	−5.5	−14.2	−28.6
d4,5 RHD	37	−4.6	−11.5	−22.8
d11,12 RHD	48	−4.7	−13.1	−27.6
d18,19 RHD	23	−4.3	−10.4	−20.1

[a] The binding constants are obtained from a fit of the binding model to the experimental binding isotherms. Each value is the mean of two independent measurements. [b] The free energy was calculated according to $\Delta G° = -RT \ln 55.5$ K. [c] Binding enthalpies are the mean of at least two independent sets of ITC experiments. [d] The entropy of binding was calculated with $\Delta G° = \Delta H° - T\Delta S°$. [e] Binding isotherms were determined with fluorescence spectroscopy. [f] Binding isotherms were determined with CD spectroscopy.

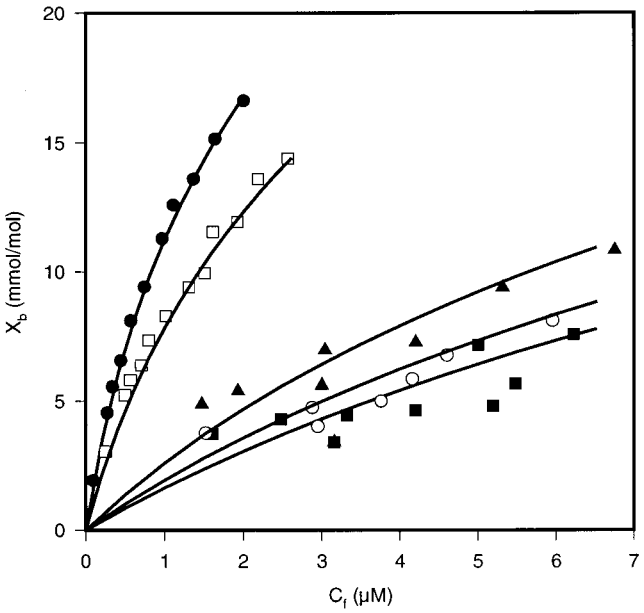

FIGURE 3: Binding isotherms of RHD and its double D-isomers for POPC/POPG (3:1) LUVs at 30 °C (buffer, 10 mM Tris and 100 mM NaCl, pH 7.4): (●) RHD, (□) d2,3 RHD, (○) d4,5 RHD, (■) d11,12 RHD, (▲) d18,19 RHD. Isotherms were determined by means of fluorescence spectroscopy. The solid lines correspond to the theoretical binding isotherms calculated by combining a surface partition equilibrium with the Gouy−Chapman theory in order to correct for the electrostatic effect.

fluorescence spectra of peptides (c^0_{pep} between 3 and 10 μM) were measured in the presence of varying amounts of LUVs (lipid−peptide ratio between 0 and 1000). From the individual fluorescence spectra, the corresponding spectrum of lipid vesicles without peptide was subtracted and the resulting spectra were corrected for the inner filter effect (*25*). The fluorescence spectra of the peptide without lipid and of the completely bound peptide were denoted $f_f(\lambda)$ and $f_b(\lambda)$, respectively. The fluorescence spectrum, $f(\lambda)$, at a specific peptide-to-lipid ratio is then given by

$$f(\lambda) = X_{P,b}\, f_b(\lambda) + (1 - X_{P,b}) f_f(\lambda) \qquad (7)$$

where $X_{P,b}$ is the mole fraction of bound peptide. A fit of eq 7 to an experimental spectrum $f(\lambda)$, measured for a specific peptide and lipid concentration, yields $X_{P,b}$. The corresponding free peptide concentration, c_f, and the molar ratio of bound peptide per lipid, X_b, can then be calculated according to eqs 3 and 4, respectively. The binding isotherms of RHD peptides for POPC/POPG (3:1) LUVs are shown in Figure 3. The isotherms of RHD and d2,3 RHD were calculated under the assumption that the peptide can cross the bilayer (lipid in the outer + inner layer), because both peptides are highly active in permeabilizing membranes (cf. below). The other double D-analogues, however, do not permeabilize membranes under the condition of the fluorescence experiments, and the binding isotherms were thus calculated on the basis of the lipid present in the outer leaflet of the vesicles only (50% of the overall lipid). The surface partition model was again employed to fit the experimental binding isotherms (cf. solid lines in Figure 3) and the corresponding binding constants K and free energies of binding $\Delta G°$, as determined from two independent measurements of the binding isotherm, are summarized in Table 2. As previously observed with other peptides (*11*, *34*), the lipid affinity of the analogues is found to be slightly smaller for LUVs than for SUVs.

Determination of the Enthalpy of Binding. The enthalpy of binding of RHD peptides to negatively charged POPC/POPG (3:1) SUVs and LUVs at 30 °C was determined by means of high-sensitivity isothermal titration calorimetry (*29*). Small aliquots of a peptide solution (30 μL of a 20−50 μM peptide solution in buffer 10 mM Tris, 100 mM NaCl, pH 7.4) were injected into an excess of lipid vesicles contained in the calorimeter cell (V_{cell} = 1.404 mL, 10 mM lipid, same buffer; experiments not shown). Because of the large lipid-to-peptide ratio and the high lipid affinity of the peptides, virtually complete peptide binding was achieved. In separate control experiments, the heat of dilution was obtained by injection of peptide into buffer. Subtraction of the heat of dilution and division by the molar amount of injected peptide yielded the molar enthalpy of binding, $\Delta H°$ (Table 2). The $\Delta H°$ values given in Table 2 are the mean of at least two independent sets of ITC experiments. Binding of the peptides to SUVs was accompanied by a distinctly exothermic interaction enthalpy of −10 to −15 kcal/mol. In contrast, the binding enthalpy of all analogues was considerably larger for LUVs (−2 to +4 kcal/mol). For both vesicle systems, the largest exothermic interaction enthalpy was found for the all L-peptide (SUVs, −14.9 kcal/mol; LUVs, −1.7 kcal/mol). $\Delta H°$ was larger for the less helical double D-isomers (d4,5; d11,12; d18,19 RHD). In the case of LUVs, the binding enthalpy even changed its sign and became positive.

Knowledge of $\Delta H°$ and $\Delta G°$ allowed a calculation of the entropy of binding $\Delta S°$ (Table 2) according to

$$\Delta S° = (\Delta H° - \Delta G°)/T \qquad (8)$$

The binding entropy opposes binding of the peptides to SUVs ($\Delta S°$ = −20.1 to −30.3 cal/mol K), but drives binding of the peptides to LUVs ($\Delta S°$ = 12.4−26.6 cal/mol K).

Peptide-Induced Membrane Permeabilization. Mitochondrial presequences perturb bilayers thereby leading to a permeabilization of the membrane and to a peptide translocation from the outer to the inner membrane monolayer (*16*, *26*, *35*). We have thus studied peptide-induced membrane permeabilzation at 30 °C using a dye release assay. In this assay, 25 μM of calcein-loaded POPC/POPG (3:1) LUVs were added to a stirred peptide solution of defined concentration. Membrane permeabilization was monitored by the increase in fluorescence due to the dilution of the self-quenched fluorescence dye calcein in the surrounding solution. Figure 4A shows the dependence of the fluorescence dequenching on the peptide concentration, measured 5 min after mixing of peptide with vesicles. All peptides were able to permeabilize negatively charged POPC/POPG (3:1) LUVs. The highly helical all-L RHD and d2,3 RHD were very potent in membrane permeabilization as assessed by the low concentration necessary to induce 50% fluorescence dequenching ($EC_{50} \approx 1.3$ μM). In contrast, the activity was reduced for the less helical double D-isomers. (EC_{50} between 12 and 30 μM).

However, it is more instructive to correlate the extent of dye release with the *bound* peptide-to-lipid ratio, X_b (Figure 4B). The X_b values corresponding to 50% fluorescence dequenching are very similar for all analogues (between 10

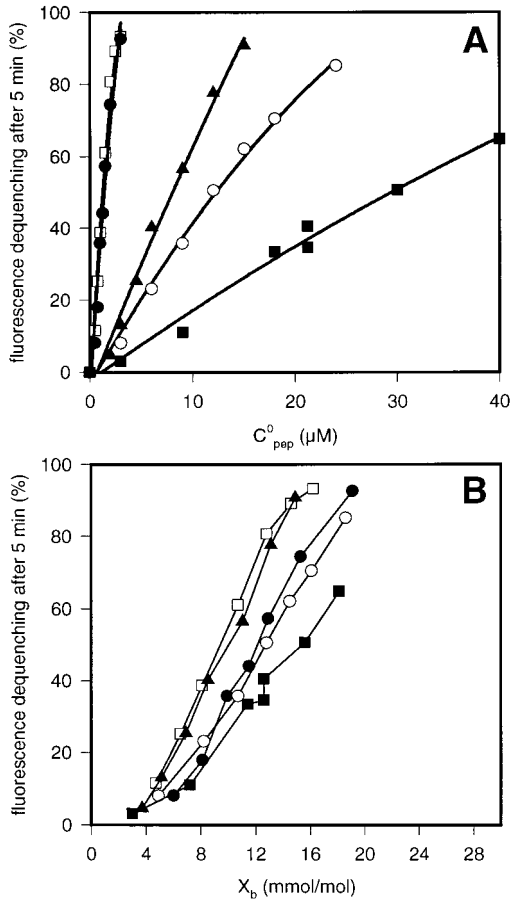

FIGURE 4: Peptide-induced dye release from calcein-loaded POPC/POPG (3:1) LUVs at 30 °C: (●) RHD, (□) d2,3 RHD, (○) d4,5 RHD, (■) d11,12 RHD, (▲) d18,19 RHD. (A) Dependence of the fluorescence dequenching after 5 min on the peptide concentration (buffer: 10 mM Tris, 100 mM NaCl, pH 7.4). The lipid concentration was 25 μM. (B) Relationship between calcein leakage and the ratio of bound peptide per lipid, X_b, as calculated by combining the binding isotherms (Figure 3) with the results of the dye release experiments (Figure 4A).

and 15 bound peptide molecules/1000 lipid molecules). Furthermore, no correlation exists between the peptide helicity and the amount of bound peptide necessary to permeabilize the membrane, indicating that peptide helicity is not a structural requirement for membrane perturbation.

DISCUSSION

In the present study, we have analyzed the role of helix formation for membrane-binding and perturbation of a peptide corresponding to the presequence of rat mitochondrial rhodanese (RHD). The 23-amino acid peptide RHD assumes a random coil conformation in aqueous solution but folds into an amphipathic α-helix in 50% trifluoroethanol (79% α-helix) or when bound to a lipid membrane (70% α-helix; Table 1, Figure 1). To quantitatively determine the contribution of helix formation to membrane-binding and perturbation, we synthesized four double D-isomers. As expected, double D-substitution resulted in a local disturbance of the α-helix as revealed by a reduced helicity of these analogues in TFE and in the membrane-bound state (Table 1). While the decrease in helicity compared to the all-L peptide is only 3% for the lipid-bound d2,3 RHD, it is between 26 and 28% for the other D,D analogues. The small effect of double

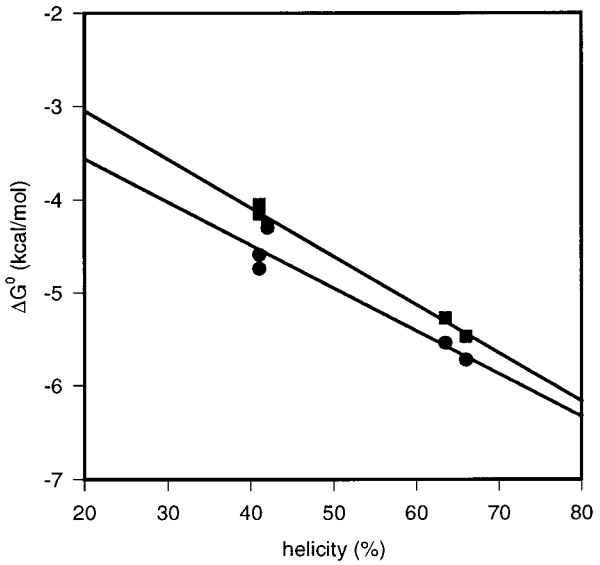

FIGURE 5: Correlation of the free energy of binding, $\Delta G°$, of RHD peptides to POPC/POPG (3:1) SUVs (●) and LUVs (■) with the helicity. The solid lines correspond to the linear regression of the experimental data (cf. text).

D-substitution in position 2 and 3 indicates that the RHD helix is considerably frayed in this region. This is in agreement with a NMR study of RHD bound to dodecylphosphocholine micelles, suggesting a helical stretch between amino acids 2 and 22 (*6*). However, the residues up to position 4 were poorly shielded from amide proton exchange, ruling out the existence of a stable helix for the first few residues (*6*).

Binding of RHD and its double D-isomers to small (SUVs) and large (LUVs) unilamellar vesicles was studied by CD and fluorescence spectroscopy, respectively (Figures 2 and 3). For both model systems, the parent peptide was found to have the highest lipid affinity. The affinity was only little reduced for the d2,3 analogue, but considerably smaller for the other double D-isomers. As reported previously for other peptides, the lipid affinity of all analogues was somewhat larger for SUVs than for LUVs (*11*, *34*). Binding of peptides to the vesicles was quantitatively described by a model which combines a surface partition equilibrium with the Gouy−Chapman theory in order to correct for the electrostatic attraction of the positively charged RHD analogues ($z \sim +2.5$ at pH 7.4) to the negatively charged membrane surface (for binding constants K and free energies of binding $\Delta G°$, see Table 2) (*28*, *29*). As recently shown for the antibacterial peptide magainin (*9*, *11*), it is possible to correlate the standard free energy of binding with the change in helicity upon membrane-binding (Figure 5). Linear regression analysis yields the following expression for SUVs:

$$\Delta G° = -0.20 n_{helix} - 2.6 \text{ (kcal/mol)}; \; r^2 = 0.92$$

and for LUVs

$$\Delta G° = -0.23 n_{helix} - 2.0 \text{(kcal/mol)}; \; r^2 = 0.99$$

where n_{helix} is the number of helical residues within the peptide. The contribution of helix formation to the free energy of binding can be obtained from the slope of the regression lines, i.e., $\Delta G_{helix} = -0.20$ kcal/mol/residue for

SUVs and $\Delta G_{helix} = -0.23$ kcal/mol/residue for LUVs. These values can be compared with data recently obtained for the antibacterial peptide magainin 2 amide (M2a) (*9*, *11*). The free energy of membrane-induced helix formation of M2a was found to be −0.14 (−0.12) kcal/mol/residue for SUVs (LUVs). Both peptides, RHD and M2a, consist of 23 amino acids and are able to form an amphipathic α-helix. However, there exists no sequence homology between M2a and RHD. Nevertheless, the free energy of helix formation is similar for both peptides.

From the intercept of the $\Delta G°$-versus-helicity plot, the free energy of binding of a hypothetical nonhelical peptide is calculated to be $\Delta G°_{coil} = -2.6$ kcal/mol for SUVs and −2.0 kcal/mol for LUVs. A comparison of the latter values with the overall free energy of binding (SUVs, $\Delta G° = -5.7$ kcal/mol; LUVs, $\Delta G° = -5.5$ kcal/mol) reveals that helix formation contributes −3.1 kcal/mol (54%) to the free energy of binding to SUVs and −3.5 kcal/mol (64%) to the free energy of binding to LUVs. Again, these values are in remarkable agreement with the data observed for M2a, where helix formation accounted for about 50% of the free energy of binding (*9*, *11*). Therefore, as previously suggested for M2a, helix formation is a major driving force for membrane-binding of the mitochondrial presequence RHD.

A second major contribution to the free energy of binding arises from the hydrophobic effect, i.e., the burial of hydrophobic peptide side chains into the hydrophobic interior of the lipid membrane (*36*).

Isothermal titration calorimetry was used to study the enthalpy of membrane-binding of RHD and its double D-isomers. Figure 6A shows a plot of $\Delta H°$ versus the helicity of the peptides for SUVs and LUVs. For all analogues, $\Delta H°$ was distinctly larger for LUVs than for SUVs. A similar dependence of $\Delta H°$ on the vesicle type has recently been observed for M2a and its double D-isomers (*11*, *37*). For each vesicle system, the enthalpy of binding was lower for RHD and d2,3 RHD than for the less helical double D-isomers. To determine the enthalpy of helix formation, a linear regression analysis between $\Delta H°$ and the helicity was performed. However, the scatter of the enthalpy values was considerable and the quality of the linear regression was rather poor yielding for SUVs:

$$\Delta H° = -0.53 n_{helix} - 6.6 \text{ (kcal/mol)}; \; r^2 = 0.71$$

and for LUVs

$$\Delta H° = -0.63 n_{helix} + 8.8 \text{ (kcal/mol)}; \; r^2 = 0.74$$

From the slopes of the regression plots, the enthalpy of helix formation was determined to be −0.53 and −0.63 kcal/mol/residue for SUVs and LUVs, respectively. A similar result was recently obtained for M2a (−0.7 and −0.8 kcal/mol/residue, $r^2 = 0.97$) (*9*, *11*). A linear relation is generally expected, if the enthalpy of helix formation is the same for each helical segment within a peptide chain. This is strictly valid only for homopolymers in an isotropic solvent. The value of ΔH_{helix} of −0.5 to −0.6 kcal/mol/residue for membrane-bound RHD should hence be considered as an approximate value averaged over different positions within the peptide chain. From the $\Delta S°$ versus helicity plot (not shown), ΔS_{helix} was calculated to be between −1.0 and −1.4 cal/mol K/residue, which is again similar to the value previously found for M2a (SUVs, −1.9 cal/mol K/residue; LUVs, −2.3 cal/mol K) (*9*, *11*). It is interesting to note that despite the large differences in the $\Delta H°$ and $\Delta S°$ of *binding* for SUVs and LUVs, the thermodynamic parameters of *helix* formation were very similar for the two types of vesicles.

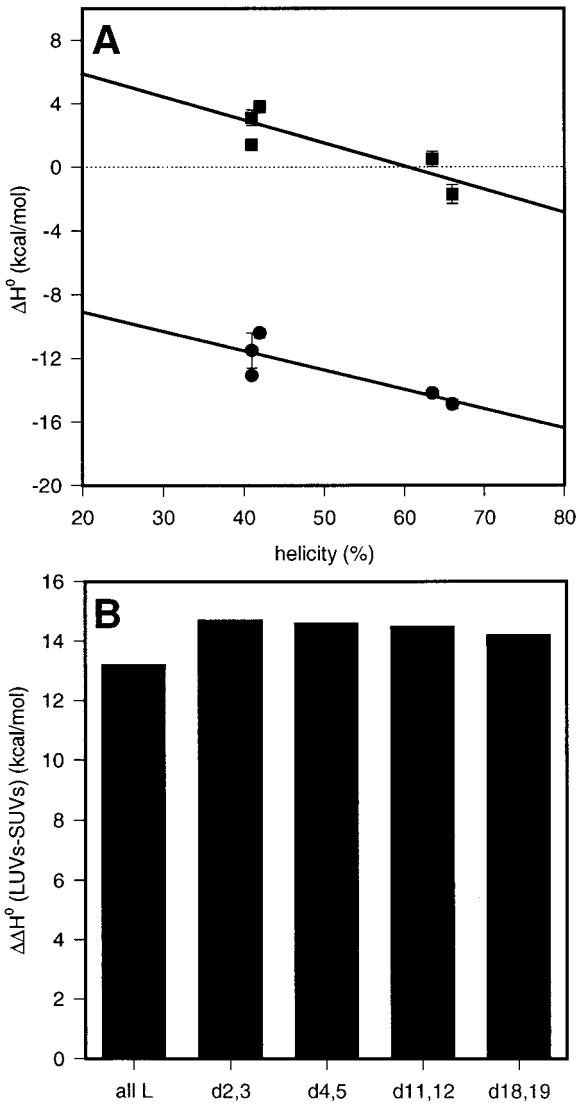

FIGURE 6: (A) Variation of the enthalpy of binding, $\Delta H°$, of RHD peptides for POPC/POPG (3:1) SUVs (●) and LUVs (■) with the helicity. The solid lines correspond to the linear regression of the experimental data (cf. text). (B) Difference in the binding enthalpies for SUVs and LUVs, $\Delta\Delta H°$, of the individual analogues.

It is instructive to compare ΔH_{helix} and ΔS_{helix} in a membrane environment with the corresponding parameters of peptides in water. In water, ΔH_{helix} was found to be in the range of −0.9 to −1.3 kcal/mol/residue (*24*, *38*−*42*), which is more exothermic than in a membrane (−0.5 to −0.8 kcal/mol/residue). The enthalpy of helix formation in water was largely independent of the peptide sequence and was mainly attributed to the formation of intramolecular hydrogen bonds (*40*, *42*). In the more hydrophobic environment of water/trifluoroethanol mixtures, ΔH_{helix} was distinctly less exothermic than in water and the enthalpy increased with increasing trifluoroethanol content (between −0.9 kcal/mol in 1 M TFE and −0.1 kcal/mol/residue in pure TFE) (*43*). The data available so far indicate that α-helix formation in a more hydrophobic environment (organic solvent, mem-

brane) is characterized by a smaller exothermic enthalpy change than in water. The same holds true for the entropy of helix formation. Typical residual ΔS_{helix} values in water range between −2.5 and −4.6 cal/mol K (*39*, *40*, *44*), while the values are distinctly less negative (between −1.0 and −2.3 cal/mol K/residue) in a membrane.

A comparison of the thermodynamic data for *binding* to SUVs and LUVs reveals only minor differences in the $\Delta G°$ values but large differences in $\Delta H°$ and $\Delta S°$ providing evidence for an entropy-enthalpy compensation mechanism which is, however, independent of helix formation. If the regression plots (Figures 5 and 6A) are extrapolated to zero percent helicity, the binding parameters of a hypothetical, nonhelical peptide are derived as $\Delta H° \approx -7$ kcal/mol and $\Delta S° \approx -13$ cal/mol K for SUVs. In contrast, binding to LUVs is driven by a large positive entropy of $\Delta S° \approx 36$ cal/mol K and strongly opposed by a positive enthalpy change of $\Delta H° \approx \sim 9$ kcal/mol. On the basis of the extrapolation in Figure 6A, the enthalpy difference between LUVs and SUVs is estimated as $\Delta\Delta H° = 15.4$ kcal/mol. $\Delta\Delta H°$ can also be evaluated for each peptide individually and yields 14.2 ± 0.6 kcal/mol (on residual basis, 0.62 ± 0.03 kcal/mol) (Figure 6B). The corresponding value for M2a and its double D-isomers was $\Delta\Delta H° = 14.3 \pm 0.6$ kcal/mol (normalized to one residue, 0.62 ± 0.03 kcal/mol) (*9*, *11*), in remarkable agreement with the present study. In the course of our studies with peptides and proteins of different size, the binding enthalpy difference, $\Delta\Delta H°$, between SUVs and LUVs was always found to be highly constant, i.e., 0.6 ± 0.1 kcal/mol if calculated on the basis of one amino acid residue (Wieprecht and Seelig, unpublished results). The high resemblance of the $\Delta\Delta H°$ for M2a, RHD, their double D-isomers and other amphipathic peptides/proteins suggests that the differences in $\Delta H°$ (and also in $\Delta S°$) between SUVs and LUVs are not dependent on the specific amino acid sequence and on the peptide conformation, but depend rather on differences in the packing and lipid structure between the two frequently employed model systems (*11*, *34*, *37*). SUVs with a diameter of ∼30 nm are relatively loosely packed because of their small radius and the resulting high curvature. This enhances the lipid flexibility and leads to comparably small cohesive forces (van der Waals attraction) between the lipid molecules. In contrast, 100 nm LUVs are well packed and strong cohesive forces exist between the lipid molecules. These structural differences probably account for the observed differences in the thermodynamic binding parameters. However, before final conclusions about the molecular basis of these differences can be drawn, additional investigations are necessary which are currently underway in our laboratory.

Mitochondrial presequences were previously shown to perturb lipid bilayers. Bilayer perturbation results in an enhanced membrane permeability (*16*, *35*) and in a translocation of peptides from the outer to the inner leaflet of vesicles (*26*). Whether the membrane perturbation potential plays a role for the biological function is not clear at present. We have used a dye-releasing assay to study the potential of RHD and its analogues to perturb bilayers. All analogues were able to induce dye release from calcein-loaded vesicles. The activity was largest for RHD and d2,3 RHD, but was significantly reduced for the other double D-analogues. Indeed, the order of activity followed the order of the lipid affinity and helicity (Figure 4A). A correlation between the ratio of bound peptide per lipid X_b with the dye-releasing activity revealed that the enhancement of membrane permeability per unit of bound peptide is similar for all analogues. Equally important, no correlation between helicity and membrane-permeabilizing efficiency appears to exist. Hence, while helix formation plays a major role for the lipid affinity of the peptides, it is of no importance for the ability of the peptide to perturb the membrane.

One mechanism frequently suggested for membrane-permeabilizing peptides is the pore-formation mechanism (*27*, *45*). The mechanism assumes the transient formation of a transmembranaous pore consisting of associated peptide helices (sometimes separated by lipids between the helices) which are oriented perpendicular to the membrane. The stability of a pore is expected to be significantly decreased for peptides with a reduced helicity. The absence of a major effect of double D-substitution on the membrane-permeabilizing efficiency of the RHD analogues strongly suggests that an unspecific membrane perturbation rather than pore formation is the dominant mechanism. RHD and its double D-analogues bind initially only to the outer monolayer of the membrane. At a bound peptide-to-lipid ratio, X_b, of 0.013, the increase in the area of the outer monolayer amounts to about 5% [0.013 × 250 Å^2 (peptide area)/68 Å^2 (lipid area) = 0.05]. This leads to a considerable mismatch in the areas of the outer and inner monolayers and hence to membrane tension. Membrane tension can be relieved by peptide translocation to the inner leaflet. Peptide translocation is accompanied by an enhanced membrane permeability, since it involves also the transport of the hydrophilic peptide groups across the membrane.

CONCLUSION

We have investigated the role of helix formation for membrane binding and perturbation of the mitochondrial presequence RHD using the double D-amino acid approach. Binding of RHD to lipid vesicles is accompanied by a transition from a random coil to an α-helical conformation. Membrane-induced helix formation was found to be driven by an enthalpy, $\Delta H°$, of ∼−0.5 to −0.6 kcal/mol/residue but opposed by entropy, $\Delta S°$, of ∼−1.0 to −1.4 cal/mol K/residue for both large and small unilamellar vesicles. The contribution of helix formation to the free energy of binding was about −0.2 kcal/mol/residue and accounted for about 50− 60% of the overall free energy. Hence, helix formation is a major driving force for the binding reaction. While the free energy of binding of RHD and its analogues was very similar for LUVs and SUVs, the binding enthalpy and entropy was distinctly larger for LUVs than for SUVs. These differences are probably caused by differences in the lipid packing in both model systems. While helicity plays a major role for the binding reaction, it is not important for the membrane perturbation potential of the bound peptides.

REFERENCES

1. Segrest, J. P., Jackson, R. L., Morrisett, J. D., and Gotto, A. M., Jr. (1974) *FEBS Lett 38*, 247−58.
2. Wald, J. H., Krul, E. S., and Jonas, A. (1990) *J. Biol. Chem. 265*, 20037−43.
3. Wieprecht, T., Dathe, M., Schümann, M., Krause, E., Beyermann, M., and Bienert, M. (1996) *Biochemistry 35*, 10844−53.

4. Roise, D., and Schatz, G. (1988) *J. Biol. Chem. 263*, 4509−11.
5. Martin, I., Dubois, M. C., Defrise-Quertain, F., Saermark, T., Burny, A., Brasseur, R., and Ruysschaert, J. M. (1994) *J. Virol. 68*, 1139−48.
6. Hammen, P. K., Gorenstein, D. G., and Weiner, H. (1996) *Biochemistry 35*, 3772−81.
7. Gazzara, J. A., Phillips, M. C., Lund-Katz, S., Palgunachari, M. N., Segrest, J. P., Anantharamaiah, G. M., and Snow, J. W. (1997) *J. Lipid Res. 38*, 2134−46.
8. Anantharamaiah, G. M., Jones, J. L., Brouillette, C. G., Schmidt, C. F., Chung, B. H., Hughes, T. A., Bhown, A. S., and Segrest, J. P. (1985) *J. Biol. Chem. 260*, 10248−55.
9. Wieprecht, T., Apostolov, O., Beyermann, M., and Seelig, J. (1999) *J. Mol. Biol. 294*, 785−94.
10. Rothemund, S., Beyermann, M., Krause, E., Krause, G., Bienert, M., Hodges, R. S., Sykes, B. D., and Sonnichsen, F. D. (1995) *Biochemistry 34*, 12954−62.
11. Wieprecht, T., and Seelig, J. (2000) Unpublished results.
12. Ladokhin, A. S., and White, S. H. (1999) *J. Mol. Biol. 285*, 1363−9.
13. Massey, J. B., Gotto, A. M., Jr., and Pownall, H. J. (1979) *J. Biol. Chem. 254*, 9559−61.
14. Ploegman, J. H., Drent, G., Kalk, K. H., and Hol, W. G. (1978) *J. Mol. Biol. 123*, 557−94.
15. Voos, W., Martin, H., Krimmer, T., and Pfanner, N. (1999) *Biochim. Biophys. Acta. 1422*, 235−54.
16. Roise, D., Horvath, S. J., Tomich, J. M., Richards, J. H., and Schatz, G. (1986) *EMBO J. 5*, 1327−34.
17. Schleiff, E., and Turnbull, J. L. (1998) *Biochemistry 37*, 13043−51.
18. Schleiff, E., Heard, T. S., and Weiner, H. (1999) *FEBS Lett. 461*, 9−12.
19. Hartl, F. U., and Neupert, W. (1990) *Science 247*, 930−8.
20. Hammen, P. K., Gorenstein, D. G., and Weiner, H. (1994) *Biochemistry 33*, 8610−7.
21. Hope, M. J., Bally, M. B., Webb, G., and Cullis, P. R. (1985) *Biochim. Biophys. Acta. 812*, 55−65.
22. Böttcher, C. J. F., van Gent, C. M., and Pries, C. (1961) *Anal. Chim. Acta. 24*, 203−204.
23. Wiseman, T., Williston, S., Brandts, J. F., and Lin, L. N. (1989) *Anal. Biochem. 179*, 131−7.
24. Scholtz, J. M., Qian, H., York, E. J., Stewart, J. M., and Baldwin, R. L. (1991) *Biopolymers 31*, 1463−70.
25. Lakowicz, J. R. (1983) *Principles of Fluorescence Spectroscopy*, Plenum Press, New York.
26. Maduke, M., and Roise, D. (1993) *Science 260*, 364−7.
27. Matsuzaki, K., Murase, O., Fujii, N., and Miyajima, K. (1995) *Biochemistry 34*, 6521−6.
28. Seelig, J., Nebel, S., Ganz, P., and Bruns, C. (1993) *Biochemistry 32*, 9714−21.
29. Seelig, J. (1997) *Biochim. Biophys. Acta 1331*, 103−16.
30. McLaughlin, S. (1977) *Curr. Top. Membr. Transp. 9*, 71−144.
31. McLaughlin, S. (1989) *Annu. Rev. Biophys. Biophys. Chem. 18*, 113−36.
32. Aveyard, R., and Haydon, D. A. (1973) *An introduction to the principles of surface chemistry*, Cambridge University Press, London.
33. Cantor, C. R., and Schimmel, P. R. (1980) *Biophysical Chemistry*, Vol. 1, pp 283, Freeman, San Francisco.
34. Beschiaschvili, G., and Seelig, J. (1992) *Biochemistry 31*, 10044−53.
35. Zardeneta, G., and Horowitz, P. M. (1992) *J. Biol. Chem. 267*, 24193−8.
36. Tanford, F. (1980) *The hydrophobic effect: formation of micelles and biological membranes*, Wiley & Sons, New York.
37. Wieprecht, T., Apostolov, O., and Seelig, J. (2000) *Biophys. Chem. 85*, 187−198.
38. Chou, P. Y., and Scheraga, H. A. (1971) *Biopolymers 10*, 657−80.
39. Hermans, J., Jr. (1966) *J. Phys. Chem. 70*, 510−5.
40. Ooi, T., and Oobatake, M. (1991) *Proc. Natl. Acad. Sci. U.S.A. 88*, 2859−63.
41. Rialdi, G., and Hermans, J., Jr. (1966) *J. Am. Chem. Soc. 88*, 5719−20.
42. Scholtz, J. M., Marqusee, S., Baldwin, R. L., York, E. J., Stewart, J. M., Santoro, M., and Bolen, D. W. (1991) *Proc. Natl. Acad. Sci. U.S.A. 88*, 2854−8.
43. Luo, P., and Baldwin, R. L. (1997) *Biochemistry 36*, 8413−21.
44. Scholtz, J. M., and Baldwin, R. L. (1992) *Annu. Rev Biophys. Biomol. Struct. 21*, 95−118.
45. Matsuzaki, K., Murase, O., Fujii, N., and Miyajima, K. (1996) *Biochemistry 35*, 11361−8.

BI001774V